한국전산구조공학회
1998년도 봄학술발표회 논문집

Experimental Verification of Crack Detection Model using Vibration Measurement
(진동실험에 의한 균열발견모델의 실험적 검증)

김 정 태* 류 연 선** 송 철 민*** 조 현 만***
Kim, Jeong-Tae Ryu, Yeon-Sun Song, Chul-Min Cho, Hyun-Man

ABSTRACT

In this paper, a newly derived formulation of a crack detection model is presented and its feasibility to detect cracks in structures is verified experimentally. To meet this objective, the following approach is utilized. Firstly, the crack detection scheme which consists of the damage localization model and the crack detection model is formulated. Secondly, the feasibility and practicality of the complete procedure of the crack detection model is evaluated by locating and sizing cracks in clamped-clamped beams for which a few modal parameters were measured for sixteen uncracked and cracked states. Major results observed from the crack detection exercises include that for most damage cases, the predicted crack locations falls within very close to the inflicted locations of cracks in the test beam and the size of crack values estimated at the predicted locations are very close to the inflicted magnitudes.

1. INTRODUCTION

An accurate and reliable capability of damage detection in critical structural members is the key to ensure the structural safety. Often, damage that is not disclosed in those members results in failures of the structural systems and catastrophic disasters such as loss of lives, human suffering, and expenses of properties. During the past decade, a significant amount of research has been conducted in the area of damage detection via changes in modal responses of a structure. Research studies have related changes in eigenfrequencies to changes in structural properties,[1] formulated the first-order perturbation theories to identify the effect of defects in structural systems from changes in eigenfrequencies,[2] attempted to monitor and diagonize the integrity of structural systems such as bridges.[3] More recently, research efforts have been focued on investigating the feasibility of detecting damage in civil engineering structures using damage indices which are designed to implement system identification techniques to changes in dynamic modal responses of structural systems.[4,5] Despite these combined efforts, there are still outstanding needs: e.g., to locate damage and size the magnitude of damage in structures with limited modal information.

In this paper, we propose a crack detection model which is a newly derived formulation to predict the geometrical sizes of damage (i.e., crack) in structures. In order to achieve the objective, we perform the following two tasks: (1) we outline the crack detection scheme which consists of the damage localization model based on system identification using changes in dynamic modal parameters and the crack detection model based on application of changes in modal responses of structures to the first-order perturbation theory and LEFM-based crack theory, (2) we verify the feasibility and practicality of the complete procedure of the crack detection model by locating and sizing cracks in continuous beams for which a few modal parameters were measured for sixteen uncracked and cracked states. The structure type examined here are both-ends-clamped beams which were tested in PKNU laboratory.

* 부경대학교 해양공학부 조교수
** 부경대학교 해양공학부 교수
*** 부경대학교 해양공학부 연구조교

2. THEORY OF APPROACH

The crack detection scheme outlined here yields information on the location and geometrical sizes of cracks directly from changes in dynamic modal parameters of structures. A series of steps designed to satisfy the objective are schematized in Fig. 1. We predict potential locations of crack by implementing modal data of uncracked (undamaged) and cracked structures into the damage localization model. Once the crack locations are decided, then we quantify the geometrical crack sizes at the predicted locations. Modal data of undamaged and damaged structures are measured from experimental modal tests (but the undamaged modal data may be identified analytically if the initial modal are not available).

2.1 Damage Localization Model for Euler-Bernoulli Beam [References 4 and 5]

For an arbitrary homogeneous one-dimensional beam with *ne* members (in the finite element sense) and *n* nodes, a damage localization indicator for each potential damage location *j* and mode *i* as follows (assumming the beam behaves linearly):

$$\beta_{ji} = \frac{k_j}{k_j^*} = \frac{\left(\int_j \left[\phi_i''^*(x)\right]^2 dx + \int_o^L \left[\phi_i''^*(x)\right]^2 dx\right)}{\left(\int_j \left[\phi_i''(x)\right]^2 dx + \int_o^L \left[\phi_i''(x)\right]^2 dx\right)} \frac{\int_o^L \left[\phi_i''(x)\right]^2 dx}{\int_o^L \left[\phi_i''^*(x)\right]^2 dx} = \frac{NUM_{ji}}{DEN_{ji}} \tag{1}$$

in which $\phi_i(x)$ and $\phi_i^*(x)$ are the pre-damage and post-damage *j*th mode shape vectors, and k_j and k_j^* are the pre-damage and post-damage bending stiffness of *j*th element. To account for all available modes we form a single indicator for each location as

$$\beta_j = \frac{\sum_i NUM_{ji}}{\sum_i DEN_{ji}} \tag{2}$$

We then normalize the values of the indicator according to the rule

$$Z_j = (\beta_j - \mu_{\beta j})/\sigma_{\beta j} \tag{3}$$

in which $\mu_{\beta j}$ and $\sigma_{\beta j}$ are the mean and the standard deviation of the collection of β_j values.

Next, the Z_j, are classified into damaged or undamaged patterns via a statistical pattern recognition technique using hypothesis testing. The null hypothesis (i.e., H_0) is: the structure is not damaged at the *j*th location. The alternate hypothesis (i.e., H_1) is: the structure is damaged at the *j*th location. The decision rule for assigning damage to location *j* is as follows [6]:

$$\begin{aligned} &\textbf{Choose } \mathbf{H_1}\textbf{: when } \mathbf{Z_j \geq K} \\ &\textbf{Choose } \mathbf{H_0}\textbf{: when } \mathbf{Z_j < K} \end{aligned} \tag{4}$$

in which K is a number that reflects the level of significance of the test.

2.2 Formulation of Crack Detection Model

The change in eigenfrequencies of a structure due to the geometrical deviations (e.g., a crack in Fig. 2) can be computed by considering the geometrical changes as perturbations of an undisturbed geometry. Furthermore,the eigenfrequency changes are dependent on the strain energy of a static solution which is easily obtainable for small cracks and other small cut-outs [1].

With reference to Fig. 2, suppose we are given an undisturbed (i.e., undamaged) *mdof* model of a structure which yields *i*th eigenfrequencies ω_i and mode shapes ϕ_i by solving the equation

$$(\mathbf{k} - \omega_i^2 \mathbf{m})\phi_i = 0 \tag{5}$$

Also, the ith modal stiffness $K_i(=\phi_i^T\mathbf{k}\phi_i)$ and the ith modal mass $M_i(=\phi_i^T\mathbf{m}\phi_i)$ are related as

$$K_i = \omega_i^2 M_i \tag{6}$$

in which $\mathbf{k}$ and $\mathbf{m}$ represent the system stiffness and mass matrices.

Next, assume that at some later time the structure is damaged (i.e., geometrical changes due to cracks as shown in Fig. 1) in one or more locations in the structure. Let the subsequently damaged structure be characterized by the asterisk. Then analogous to the above Eq. (1), the resulting characteristic equation of the damaged structure yields eigenfrequencies ω_i^* and mode shapes ϕ_i^* of the ith mode by

$$K_i^* = \omega_i^{*2} M_i^* \tag{7}$$

in which $K_i^*(=\phi_i^{*T}\mathbf{k}^*\phi_i^*)$ is the ith modal stiffness and $M_i^*(=\phi_i^{*T}\mathbf{m}^*\phi_i^*)$ is the ith modal mass of the damaged structure.

If we relate the ith modal stiffness K_i to the ith modal strain energy W_i for the undamaged structure and K_i^* to W_i^* for the cracked structure, the ith modal strain energy loss, $\Delta W_i(=W_i^* - W_i)$, due to the crack (i.e., the strain energy for the correction of the geometry) can be computed by

$$\frac{\Delta W_i}{W_i} = \frac{\Delta K_i}{K_i} \tag{8}$$

in which $\Delta K_i(=K_i^* - K_i)$ is the change in the ith modal stiffness which represents the ith modal strain energy loss and $\Delta W_i/W_i$ represents the fraction of the ith modal strain energy (i.e., strain energy change rate) between the undamaged structure and the cracked structure. Also, On expanding and rearranging Eq. (2)-Eq. (4), we obtain

$$\frac{\Delta K_i}{K_i} = \frac{\Delta\omega_i^2}{\omega_i^2}\left(1 - \frac{\Delta M_i}{M_i}\right) + \frac{\Delta M_i}{M_i} \tag{9}$$

where ΔM_i is the change in the ith modal mass and $\Delta\omega_i^2$ is the change in eigenvalues before and after the crack.

By assuming no volume changes due to the crack and also considering a first order approximation, we ignore the ith modal mass in the solution of Eq. (5). Then on relating the strain energy change rate to the eigenfrequency changes, we obtain

$$\frac{\Delta W_i}{W_i} \approx \frac{\Delta\omega_i^2}{\omega_i^2} \tag{10}$$

Crack Detection Model for Euler-Bernoulli Beam

If the Euler-Bernoulli beam theory is used, the strain energy W_i can be written as

$$W_i = \int_0^L \frac{1}{2} EI\left\{\phi_i''(x)\right\}^2 dx \tag{11}$$

in which EI is the flexural rigidity (E is Young's modulus and I is the second moment of area), L is the length of the undamaged beam, and $\phi_i(x)$ is the mode shape function for the ith mode. Next, by implementing the energy release rate based on LEFM and assigning plane strain condition to the cracked beam and, we obtain

$$\frac{\partial\Delta W_i}{\partial a} = t\frac{(1-\nu^2)}{E}K_I^2 \tag{12}$$

in which t is the thickness of the beam, ν is Poisson's ratio, and K_I is the stress intensity factor depending on crack size a, beam dimension (e.g., thickness t, height H and length L as shown in Fig. 1), and applied flexural stress level σ. For small-crack cases, the stress intensity factor of the edge-crack in the beam (e.g., as shown in Fig. 1) is given by:

$$K_I = F(a/H)\,\sigma\sqrt{\pi a} \tag{13}$$

in which $F(a/H)$ is the geometrical factor depending on crack depth ratio a/H. Substituting Eq. (10) into Eq. (9) and further integrating Eq. (9) over the crack contour generates

$$\Delta W_i = \left(\frac{\pi t (1-\nu^2)}{2E} F^2 \sigma_k^2 a_k^2 \right)_i \tag{14}$$

in which, for the ith mode, a_k $(=a(x_k))$ represents the crack size at location x_k and σ_k $(=\sigma(x_k))$ represents the maximum flexural stress at location x_k along the beam's longitudinal axis.

For the Euler-Bernoulli beam, the stress level is given by

$$\sigma(x_k) = \frac{1}{2} E H \phi_i''(x_k) \tag{15}$$

On substituting Eq. (11) - Eq. (15) into Eq. (10), we obtain

$$\frac{\Delta\omega_i^2}{\omega_i^2} = \frac{\pi t (1-\nu^2)}{4} \frac{H^2}{I} F^2 S_{ik} a_k^2 \tag{16}$$

and

$$S_{ik} = \int_k \{\phi_i''\}^2 dx \Big/ \int_o^L \{\phi_i''\}^2 dx \tag{17}$$

in which S_{ik} represents the contribution of the kth location to the ith modal strain energy (i.e., the modal sensitivity of the ith mode and the kth location).

If the beam section is rectangular, Eq. (16) can be written in a simple form

$$\frac{\Delta\omega_i^2}{\omega_i^2} = \eta S_{ik} \left(\frac{a_k}{H} \right)_i^2 \tag{18}$$

and

$$\eta = 3\pi(1-\nu^2)(H/L)F^2 \tag{19}$$

in which $(a_k/H)_i$ is the nondimensional crack sizer at the kth location for the ith mode and η is a constant depending on beam dimensions, crack types, and possibly Poisson's ratio (note that Poisson's ratio will not be involved in Eq. (12) in the case of plane stress condition).

Equation (18) can be solved to estimate the crack sizer if the quantities $\Delta\omega_i^2/\omega_i^2$ and S_{ik} are experimentally determined or numerically generated. By considering the availability of the modal parameters measured before and after the crack initiation, the solution will be written in two forms which are either a set of resonance frequencies or a set of mode shapes. The first solution form of the crack sizer in terms of resonance frequencies is follows:

$$\left(\frac{a_k}{H} \right)_i^2 = \frac{\Delta\omega_i^2}{\omega_i^2} \frac{1}{\eta} \frac{1}{S_{ik}} \tag{20}$$

and Eq. (20) requires uncertainty-free input data of the ith resonant frequencies measured before and after the crack in order to generate a valid estimation.

Next, we derive the alternative solution form of the crack sizer in terms of mode shapes. On substituting Eq. (8) into Eq. (10) and further substituting into Eq. (18), we obtain

$$\left(\frac{a_k}{H} \right)_i^2 = \left(1 - \frac{K_i^*}{K_i} \right) \frac{1}{\eta} \frac{1}{S_{ik}} \approx \left(1 - \int_0^L (\phi_i'')^2 dx \Big/ \int_0^L (\phi_i''^*)^2 dx \right) \frac{1}{\eta} \frac{1}{S_{ik}} \tag{21}$$

in which for the Euler-Bernoulli beam, the modal stiffnesses are given as

$$K_i = \int_0^L EI(\phi_i'')^2 dx, \quad K_i^* = \int_0^L (EI)^*(\phi_i''^*)^2 dx \tag{22}$$

and by setting $K_i^* \approx \int_o^L EI(\phi_i''^*)^2 dx$, all quantities on the right-hand-side of Eq. (21) can be obtained or approximated from modal parameters derived from experimental measurements and the geometry of the structure.

3. EXPERIMENTAL VERIFICATION

3.1 Description of Test Structure

As the test structure, we selected aluminum beams with rectangular cross section of constant thickness (0.01-m), width (0.04-m), and span of 1.02-m long as shown in Fig. 2. The end conditions are clamped-clamped for both ends. The selection was made on the basis of the following reasons: (1) the beam should be long enough to allow for the validity of the theoretical assumptions used in the development of the crack detection model and (2) the geometry and boundary conditions of the beam should be appropriate to verify the crack detection model's applicability to continuous structural systems. Thus, the crack detection in beam models may show its potential application to future exercises in continuous multi-span bridges.

Here total 12 damage scenarios, which include three levels of crack inflicted at four different crack positions, were investigated as follows. Firstly, four crack locations were selected at: x/L=0.125 (Crack Loc. 1 - in which x/L denotes the dimensionless coordinate in longitudinal axis as shown in Fig. 2), x/L=0.25 (Crack Loc. 2), x/L=0.375 (Crack Loc. 3), and x/L=0.5 (Crack Loc. 4). For each location, three levels of crack sizes were simulated upon the beam as follows: a/H = 0.1 (in which a/H denotes the dimensionless crack depth), a/H = 0.2, and a/H = 0.3. The cracks in the test beams were inflicted by cuts (Fig. 2) normal to the beams' longitudinal axis, with a controlled depth. The cuts were made using a thin cutting tool. We assumed that the thickness of the cut (which is approximately 0.5mm) was carefully defined by taking into account that both sides of the crack were not supposed to make contact during the dynamic bending of the beam.

3.2 Modal Test Setup and Results

Seven sensor locations along the longitudinal direction are indicated in Fig. 3. At each location, a piezoelectric acclerometer was mounted to the middle point of beam width at the top. With the span of the test beam the seven sensors (Sensor 1 to Sensor 7 in Fig. 3) were equally spaced in the longitudinal dirction. A Dytran smart hammer provided the input impulse to the beam from the Sensor-3 position shown in Fig. 3. A signal analysis and data aquisition system was set up to measure acceleration-time histories and calculate frequency response functions and power spectra. For further modal analysis, SMS StarModal system was utilized to extract modal parameters by translating measured modal responses to fit into analytical modal responses of the test beams.

Pre-cut and post-cut accelerometer readings were taken before and after the damaging episodes. For each case, resonance frequencies of the first four bending modes are summarized in Tables 1-4. Fig. 4 shows measured mode shapes of the four modes for an uncracked beam. Also, the uncracked beam's mode shapes were compared to the corresponding mode shapes of the three crack levels (a/H = 0.1, 0.2, and 0.3) as follows: Fig. 5 shows the changes in Mode 1 when the cracks were inflicted to the location x/L=0.5 (Crack Loc. 4).

3.3 Damage Localization and Crack Detection

As a damage detection model (i.e., a mathematical representation of a structure with degrees of freedom limited corresponding to sensor readings), the Euler-Bernoulli beam model was selected. The model includes 1020 line elements of equal size between Sensor 1 to Sensor 7 (Fig. 3). Note that each element is a potential damage location and has a spacing of 1 mm or 0.1 percent (i.e., 1/1020 x 100) of the span. The use of 1-mm wide elements is justified by interpolating peuso sensor readings at the locations of 1021 nodes of the model. For each beam (either uncracked or cracked beams), mode shape functions $\phi_i(x)$, where x is the coordinate along the axis of the beam, are generated using the interpolated modal coordinates. From $\phi_i(x)$ the instantaneous curvatures $\phi_i''(x)$ are estimated. Then a

set of undamaged and damaged data of the four modes are shipped into the damage detection model.

The damage index given by Eq. (1) was used to locate damage (i.e., find the location of crack in x direction) for the twelve damage scenarios in the test beams. The criterion for the damage index which is given by Eq. (4) was established as follows: select $\mathbf{H}_0$ if $Z_i < 3$ or select $\mathbf{H}_1$ if $Z_i \geq 3$. Furthermore, the criterion was used to predict potential crack locations. Results of damage localization for the twelve damage scenarios are summarized in Table 5.

Once damage (i.e., crack) is located, the size of a crack at a predicted location is computed geometrically from the crack detection model. As stated previously, the vertical crack of opening mode of fracture gets our attention. Modal sensitivities (S_{ik}) given by Eq. (17) are generated using the mode shapes and modal curvatures previously obtained. We computed the constant η in Eq. (19) by implementing the beam dimensions previously stated, Poisson's ratio (0.33 for aluminum), and the geometrical factor (see $F(a/H)$ in Eq. (20) is approximately 1.12 for a small edge-crack).

At the kth location for the ith mode, the dimensionless crack sizer $(a_k/H)_i$ was computed by implementing the resonance frequencies of undamaged and damaged states (Table 1 to Table 4 for 12 damage scenarios), the constant η, and the modal sensitivities S_{ik} into Eq. (20). Results of crack sizers in each case at the predicted locations are summarized in Table 5.

3.4 Accuracy of Crack Detection Model

The accuracy of the crack detection scheme presented here is evaluated by measuring both the so-called localization errors and the so-called sizing errors. The localization errors le, which represent the metrical differences between real crack locations and predicted locations, are quantified by:

$$le = (\Delta x/L)100 \tag{23}$$

in which Δx is the spacing between the inflicted and predicted location and L is the reference span (i.e., 1.02 m). Also, the sizing errors, which are the differences between real depth ratio $(a/H)_r$ and predicted depth ratio $(a/H)_p$ of vertical crack, are quantified using the expression:

$$se = \left| \left((a/H)_r - (a/H)_p \right) / (a/H)_r \right| \tag{24}$$

The results on the quantification of Eq. (23) and Eq. (24) are summarized in Table 5. From the table, major results are observed as follows. Firstly, except for three damage cases, in which the localization errors are greater than one percent, most measures of the predicted crack locations falls within one percent (10mm/1020mm x 100)) error range to the inflicted cracks in the test beam. Secondly, in all predicted locations, the crack sizer estimated values very close to exact inflicted magnitudes of crack. Thirdly, the sizing errors were valued in an overall error range of 0.5~6.0 percent for all damage cases.

4. SUMMARY AND CONCLUSION

In this paper we presented a newly derived formulation of a crack detection model and its feasibility to predict the geometrical crack sizes in structures. To meet this objective, we utilized the following approach: first, we outlined the crack detection scheme which consists of the damage localization model based on system identification using changes in dynamic modal parameters and the crack detection model based on application of changes in modal responses of structures to the first-order perturbation theory and LEFM-based crack theory; second, we verified the feasibility and practicality of the complete procedure of the crack detection model by locating and sizing cracks in clamped-clamped beams for which a few modal parameters were measured for sixteen uncracked and cracked states.

From the crack detection exercises, three major results are observed as follows: (1) in most damage cases, measures of the predicted crack locations falls within very close to the inflicted cracks in the test beam; (2) in all predicted locations, the estimated crack sizes were very close to the inflicted magnitudes of crack; and (3) the sizing errors were in an error range of 0.5~6.0 percent overall for all damage cases.

5. REFERENCES

1. Gudmunson, P. *Eigenfrequency Changes of Structures Due to Cracks, Notches or Other Geometrical Changes*, J. Mech. Phys. Solids, Vol. 30, No. 5, pp. 339-353, 1982.
2. Adams, R.D., Cawley, P., Pye, C.J. and Stone, B.J. *A Vibration Technique for Non-Destructively Assessing the Integrity of Structures*, J. Mech. Engr. Science, Vol. 20, pp. 93-100, 1978.
3. Mazurek, D.F., and DeWolf, J.T. *Experimental Study of Bridge Monitoring Technique*, J. of Structural Engineering, ASCE, Vol. 116, No. 9, pp. 2532-2549, 1990.
4. Kim, J.T., and Stubbs, N. *Model-Uncertainty Impact and Damage-Detection Accuracy in Plate Girder*, J. of Structural Engineering, ASCE, Vol. 121, No. 10, pp. 1409-1417, 1995.
5. Stubbs, N., and Kim, J.T. *Damage Localization in Structures Without Baseline Modal Parameters*, AIAA Journal, AIAA, Vol. 34, No. 8, pp. 1644-1649, 1996.
6. Gibson, J.D., and Melsa, J.L. *Introduction to Nonparametric Detection with Applications*, Academic Press, New York, 1975.

감사의 글

이 논문은 1997년도 한국학술진흥재단의 공모과제 연구비 지원에 의해 이루어진 것으로 연구비를 지원해 준 재단당국에 감사드립니다.

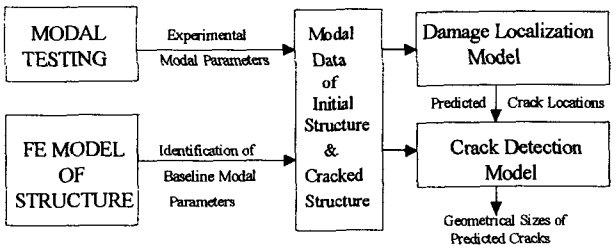

Fig. 1. Damage Localization and Crack Detection Scheme

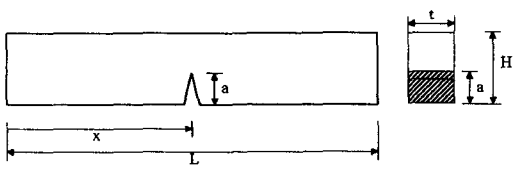

Fig. 2. Schematic of Cracked Beam

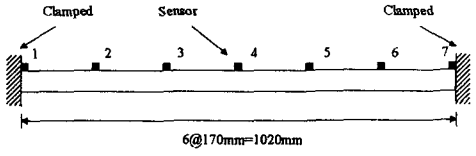

Fig. 3. Model Beam and Sensor Lay-Out

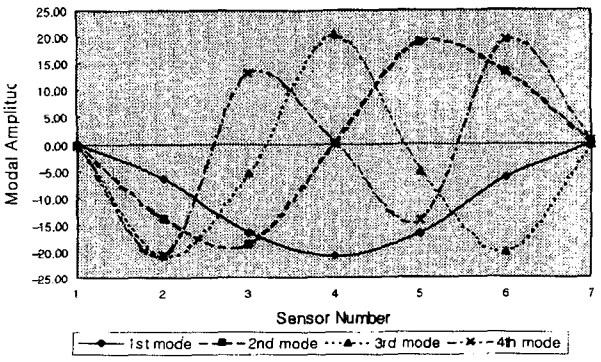

Fig. 4. Mode Shapes of Uncracked Beam

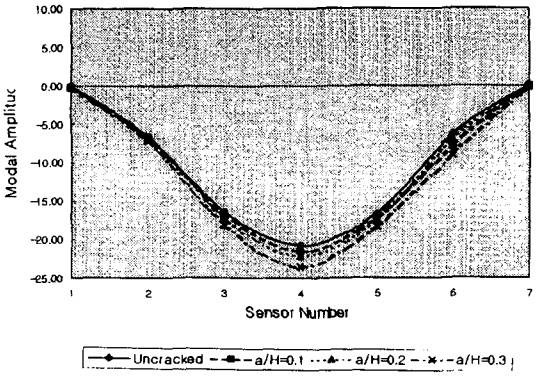

Fig. 5. Mode 1 for Uncracked and 3-Crack Levels

Table 1. Resonance Frequencies of Uncracked and 3 Cracked Cases at Crack Loc. 1

Mode No	Natural Frequency (Hz)			
	Uncracked	a/H=0.1	a/H=0.2	a/H=0.3
1	49.54	48.32	48.05	47.65
2	137.24	137.11	137.09	137.02
3	268.92	268.75	268.68	268.51
4	442.78	442.34	441.76	440.67

Table 2. Resonance Frequencies of Uncracked and 3 Cracked Cases at Crack Loc. 2

Mode No	Natural Frequency (Hz)			
	Uncracked	a/H=0.1	a/H=0.2	a/H=0.3
1	50.18	50.12	49.95	49.52
2	138.96	138.74	138.55	138.21
3	272.10	271.79	271.22	270.38
4	448.58	448.38	448.26	448.09

Table 3. Resonance Frequencies of Uncracked and 3 Cracked Cases at Crack Loc. 3

Mode No	Natural Frequency (Hz)			
	Uncracked	a/H=0.1	a/H=0.2	a/H=0.3
1	49.80	49.73	49.69	47.57
2	138.10	137.90	137.60	136.90
3	269.97	269.89	269.81	269.78
4	444.60	444.02	442.80	440.91

Table 4. Resonance Frequencies of Uncracked and 3 Cracked Cases at Crack Loc. 4

Mode No	Natural Frequency (Hz)			
	Uncracked	a/H=0.1	a/H=0.2	a/H=0.3
1	47.75	44.87	41.71	38.34
2	137.55	137.50	137.45	137.49
3	270.50	270.05	269.69	267.40
4	446.40	446.27	445.80	444.50

Table 4. Results of Crack Detection and Accuracy Quantification

Inflicted Crack(s)		Damage Localization		Crack Detection	
Location (x/L)	Magnitude (a/H)	Predicted Location (x/L)	Localization Error (%)	Predicted Size (a/H)	Sizing Error (%)
Crack Loc.1 (0.125)	0.1	0.128	0.34	0.096	4.0
Crack Loc.1 (0.125)	0.2	0.123	0.25	0.199	0.5
Crack Loc.1 (0.125)	0.3	0.127	0.24	0.308	2.7
Crack Loc.2 (0.25)	0.1	0.275	2.55	0.106	6.0
Crack Loc.2 (0.25)	0.2	0.254	0.39	0.202	1.0
Crack Loc.2 (0.25)	0.3	0.245	0.49	0.304	1.3
Crack Loc.3 (0.375)	0.1	0.362	1.32	0.099	1.0
Crack Loc.3 (0.375)	0.2	0.360	1.52	0.190	5.0
Crack Loc.3 (0.375)	0.3	0.359	1.62	0.273	6.0
Crack Loc.4 (0.5)	0.1	0.489	1.08	0.105	5.0
Crack Loc.4 (0.5)	0.2	0.490	0.98	0.206	3.0
Crack Loc.4 (0.5)	0.3	0.493	0.68	0.306	2.0